FILE COPY
No. 2

NACA

RESEARCH MEMORANDUM

CLASSIFICATION CHANGED TO ___UNCLASSIFIED___
BY AUTHORITY OF NASA CLASSIFICATION CHANGE
NOTICES, CHANGE NO. 213-33 , EFF. 4/22/71

TRANSONIC FLIGHT EVALUATION OF THE EFFECTS

OF FUSELAGE EXTENSION AND INDENTATION ON THE DRAG

OF A 60° DELTA-WING INTERCEPTOR AIRPLANE

By Edwin J. Saltzman and William P. Asher

High-Speed Flight Station
Edwards, Calif.

NATIONAL ADVISORY COMMITTEE
FOR AERONAUTICS
WASHINGTON
September 26, 1957

6355

UNCLASSIFIED

NATIONAL ADVISORY COMMITTEE FOR AERONAUTICS

RESEARCH MEMORANDUM

TRANSONIC FLIGHT EVALUATION OF THE EFFECTS

OF FUSELAGE EXTENSION AND INDENTATION ON THE DRAG

OF A 60° DELTA-WING INTERCEPTOR AIRPLANE

By Edwin J. Saltzman and William P. Asher

SUMMARY

Lift and drag characteristics of a 60° delta-wing interceptor airplane incorporating fuselage extension and indentation have been determined in flight. The data were obtained over the Mach number range from about 0.7 to 1.15 and for altitudes of 25,000, 40,000, and 50,000 feet. These data are compared with the lift and drag characteristics of an airplane with a similar wing, but which did not incorporate modifications to indent or lengthen the fuselage, to determine whether transonic drag was reduced at high Reynolds numbers by improving the cross-sectional-area development.

The results of the investigation indicate that anticipated transonic drag reductions have been realized, the reduction amounting to about 0.0050 in drag coefficient at a Mach number of about 1.1. This reduction amounts to about 25 percent of the drag rise for the prototype airplane. The reduced transonic drag of the modified airplane resulted in an improvement in maximum lift-drag ratio of about 15 percent in the supersonic region.

There are significant changes in longitudinal trim which result in less trim drag for the modified airplane. These changes in trim amount to from 1° to 2° less control deflection needed by the modified airplane at moderate lift conditions.

Three sets of comparable model data are included. These low Reynolds number tests indicated reductions in drag coefficient, due to indenting and extending the fuselage, ranging from 0.0025 to 0.0045 at a Mach number of about 1.1.

INTRODUCTION

Wind-tunnel investigations and theoretical studies have led to methods of reducing the drag of airplanes at transonic speeds. Flight tests of delta-wing interceptors at the NACA High-Speed Flight Station were initiated to determine at full scale the reductions in drag which could be achieved by smoothing the cross-sectional-area development and by cambering the leading edges of a delta wing.

The technique of smoothing the area development, popularly known as the area rule (ref. 1), has been used to improve the performance of a cambered delta-wing airplane recently tested at the High-Speed Flight Station at Edwards, Calif. Details of the resultant transonic drag reduction are presented herein.

The modifications involved in smoothing the area development consisted primarily of lengthening the fuselage to improve the fineness ratio and indenting the fuselage in the region of the wing to reduce the overall maximum cross-sectional area. The resultant configuration will henceforth be referred to as the modified airplane.

The drag characteristics of the modified airplane are compared to those of a delta-wing airplane incorporating only the cambered leading-edge improvement (fuselage extension and indentation not incorporated). Details pertaining to this configuration, referred to in this paper as the prototype airplane, are presented in reference 2.

In addition, comparison is made with unpublished data from 1/20-scale, 1/5-scale, and equivalent-body models which also incorporated fuselage extension and indentation.

SYMBOLS

A	airplane cross-sectional area, sq ft
a_l	longitudinal acceleration, g units
a_n	normal acceleration, g units
C_D	drag coefficient, D/qS
ΔC_D	difference between the minimum drag coefficient above the drag rise and the minimum drag coefficient at the beginning of the drag rise

C_L lift coefficient, L/qS

C_{L_α} lift-curve slope, deg^{-1}

C_N normal-force coefficient, Wa_n/qS

C_X longitudinal-force coefficient, $\dfrac{F_n - Wa_l}{qS}$

$\bar{c}$ mean aerodynamic chord, ft

D drag force along flight path, lb

F_j jet thrust, lb

F_n net thrust, lb

F_r ram drag, lb

g gravitational acceleration, ft/sec^2

L lift force normal to flight path, lb

$(L/D)_{max}$ maximum lift-drag ratio

l fuselage length, ft

M Mach number

P_0 ambient pressure, lb/sq ft

q dynamic pressure, $0.7M^2P_0$, lb/sq ft

R Reynolds number based on mean aerodynamic chord, $\rho V\bar{c}/\mu$

S wing area, sq ft

V true airspeed, ft/sec

W airplane weight, lb

α angle of attack, deg

δ_e effective longitudinal control deflection, $\dfrac{\delta_{e_L} + \delta_{e_R}}{2}$, deg

μ viscosity, $lb\text{-}sec/ft^2$

ρ air density, slugs/cu ft

Subscripts:

L   left

m   modified

p   prototype

R   right

AIRPLANES AND MODELS

Airplanes

The prototype airplane is a $60°$ delta-wing interceptor powered by a single turbojet engine with afterburner. The engine is supplied air through twin side inlets which join ahead of the compressor face. The airplane does not have a horizontal tail but utilizes elevons at the wing trailing edges for longitudinal control. Detailed physical characteristics of this airplane can be found in table I.

While the general physical features of the modified airplane are the same as those mentioned in the preceding paragraph, certain important details have been changed. The wing is the same with the exception of the trailing-edge reflex at the wing tips which has been reduced from $10°$ to $6°$. The fuselage has been greatly modified from that of the prototype, as can be seen in the photographs of figure 1. The overhead views of figure 1(a) show the extended nose, the indented fuselage, and the added volume at the tail cone on the modified airplane. The side views shown in figure 1(b) illustrate the fuselage extension ahead of the wing, the duct inlet changes, and the addition of tail-cone pods on the modified airplane. The vertical tail has been moved rearward about 2 feet relative to the mean aerodynamic chord and the overall increase in fuselage length is about 11 feet. The effect of these modifications on the cross-sectional-area distribution is shown in figure 2 and a comparison of the physical characteristics of the two airplanes can be seen in table I. Three-view drawings are shown for comparison in figure 3.

Models

1/20-scale models.- The two 1/20-scale models (one prototype, one modified) were tested in the Langley 8-foot transonic tunnel by Kenneth E. Tempelmeyer and Robert S. Osborne. The wings of both models were cambered similar to the full-scale wing; however, the fence at the 37-percent semispan station of the full-scale wing was not employed on the wing of either model.

The specific deviations of the models from exact models are as
follows: for the prototype model, the fuselage was 0.2 inch smaller in
diameter and the tail cone about 1.1 inch shorter than a true scale model;
for the modified airplane model, the amount of trailing-edge reflex out-
board of the elevon was 10° up instead of 6°, as on the full-scale air-
plane. In addition, this model had a shorter nose than the full-scale
airplane and it did not have pods at the tail cone or simulated air flow
through the duct system. However, rearward from the canopy the fuselage
was modified according to the same concepts as were used in modifying the
full-scale airplane.

1/5-scale models.- The two 1/5-scale models were rocket-propelled
vehicles tested at the Pilotless Aircraft Research Station by Harvey A.
Wallskog. Both models had symmetrical section wings without trailing-
edge reflex; however, both had air flow through the duct systems.

The specific deviations of the models from exact models are as
follows: for the prototype model, fences were mounted only at the
67-percent-semispan station, and, in addition, the fuselage was slightly
enlarged at the base; for the modified airplane model, there were no
fences and the nose was shorter than that of an exact model. Rearward
from the canopy the fuselage was modified according to the same concepts
as were used for the full-scale airplane.

Equivalent-body models.- The approximate 1/60-scale equivalent-body
models were bodies of revolution machined from steel and aluminum with
three hexagonal-section stabilizing fins pinned in place along the after-
body. The equivalent cross-sectional duct area was subtracted from the
body of revolution along the inlet region to the base and, in addition,
the cross-sectional area of the stabilizing fins was removed from the aft
region.

INSTRUMENTATION AND ACCURACY

Instrumentation

The modified airplane carried standard NACA recording instruments
and synchronizing timer for measuring quantities pertinent to the lift
and drag investigation. Fuel quantity (for determining the center-of-
gravity location and airplane weight) was recorded by the pilot from a
standard cockpit instrument.

Free-stream total and static pressures were obtained from points
79 inches and 71 inches, respectively, ahead of the intersection of the

nose cone and the nose boom. Angle of attack was measured by a vane located 52 inches ahead of this intersection.

Total temperature used to calculate thrust was measured by a shielded resistance-type probe located beneath the fuselage. In addition, total pressure at the compressor face was obtained by 30 probes (5 probes on each of 6 radial rakes) located immediately ahead of the compressor face. Flush static orifices located near the total-pressure survey station provided static-pressure measurements for the compressor face. Tailpipe exit total pressure was obtained by an air-cooled probe located near the nozzle exit plane of the afterburner.

Accuracy

The angle of attack was measured for the modified airplane at a point 52 inches ahead of the intersection of the nose cone with the nose boom, which was about 6 inches greater than the distance for the prototype airplane. Hence, the angle of attack as measured should experience approximately the same (or less) upwash as was encountered in the prototype airplane investigation of reference 2. Because the effects of pitching velocity and inertia loads were accounted for and the physical details of the vane-boom system are similar to those of the prototype airplane, the overall angle-of-attack accuracy is believed to be $\pm 0.25°$ at $C_L \lesssim 0.2$ and $M \approx 0.8$, the same as that for the prototype installation.

The remaining instrumentation used in the present studies is similar to that employed in the prototype airplane, hence the details pertaining to accuracy in reference 2 are valid for these tests. It is concluded that the error in drag coefficient for summary data (which were derived from faired basic data) for $C_L \lesssim 0.2$ is within 0.0010 except for the Mach number region between 0.93 and 1.02 during the drag rise where the error is greater.

METHOD

The accelerometer method was used to determine the lift and drag characteristics of the test airplane. This method employs the following equations:

$$C_L = C_N \cos \alpha - C_X \sin \alpha$$

$$C_D = C_X \cos \alpha + C_N \sin \alpha$$

where

$$C_N = \frac{Wa_n}{qS}$$

and

$$C_X = \frac{F_n - Wa_l}{qS}$$

$$= \frac{F_j - F_r - Wa_l}{qS}$$

The single-probe method was used to obtain tailpipe total pressure (used in computing F_j) and the inlet-duct method was employed in determining F_r. Details regarding these methods of drag and thrust measurement can be obtained in reference 3.

TESTS AND PRESENTATION OF BASIC DATA

The tests consisted of wind-up turns and push-downs at approximate pressure altitude levels of 25,000, 40,000, and 50,000 feet. These tests, conducted over the Mach number range from 0.70 to 1.15, covered the Reynolds number range from about 30×10^6 to 75×10^6 based on the mean aerodynamic chord. Center-of-gravity location for these tests was between 28 and 29 percent of the mean aerodynamic chord.

Some of the basic flight data for the modified airplane are presented in figure 4 which shows the variation of C_L with α for various constant Mach numbers, and in figure 5 which represents the variation of C_L with C_D for the same Mach numbers. These data and all full-scale data to follow represent the trimmed condition.

DISCUSSION OF RESULTS

Comparison With Prototype Airplane

In the following section the trim, lift, and drag characteristics for the modified and prototype airplanes are compared to determine the effect of the fuselage extension and indentation. Because the center-of-gravity position limits were the same for both airplanes, 28 to

29 percent of the mean aerodynamic chord, differences in trim control
deflections are attributable to the configuration changes comprising
the modifications; thus, it is proper to compare the data of the two
configurations at their respective trim longitudinal control deflections.
Figure 6 indicates that there are significant differences in trim
resulting in from 1° to 2° less control deflection needed by the modi-
fied airplane at positive lift. It should be noted that the modified air-
plane requires less pilot-induced trim at positive lift even though
this airplane possesses less built-in trim in the form of trailing-edge
reflex.

A comparison of the variation of C_{L_α} with Mach number is shown
for the two airplanes in figure 7. The comparison indicates close
agreement between the two configurations for lift coefficients from
0.05 to 0.30.

A significant advantage in maximum lift-drag ratio for the modified
airplane is shown in figure 8. This improvement amounts to about 15 per-
cent of $(L/D)_{max}$ for the prototype airplane in the supersonic region.
In the subsonic region the advantage of the modified airplane results
from reduced drag due to lift. The reduced drag due to lift can be
recognized in figure 9(a) by comparing the slopes of the curves for
the two airplanes. In figure 9(b) the variation of C_D with C_L is
shown for the two airplanes.

A more graphic indication of the reduction of drag attributable
to the modifications is a comparison of the variation of drag coefficient
with Mach number as shown in figure 10. The zero-lift drag for the modi-
fied airplane is slightly lower at the lowest test Mach numbers but is
essentially the same as the zero-lift drag for the prototype airplane
prior to the drag rise. In the supersonic region the zero-lift transonic
drag advantage of the modified airplane amounts to about 50 drag counts
(0.0050) at $M \approx 1.1$. This is approximately 17 percent of the supersonic
drag level of the prototype airplane or 25 percent of the prototype air-
plane drag rise. As can be seen, the transonic drag reduction is essen-
tially the same for $C_L \approx 0.2$ (a usable lift coefficient) as for zero
lift.

Comparison of Flight Results With Model Tests

It is of interest to compare the effects of greatly modifying a
configuration at full scale with the predictions of model tests at low
Reynolds number. Many models of this family of airplanes have been
tested. Unfortunately, the models of the modified airplane tested in
the transonic region do not incorporate all the external physical fea-
tures of the full-scale airplane. However, 1/20- and 1/5-scale models

with indented and extended fuselages and approximately 1/60-scale
equivalent-body models have been tested and the results of these tests
are compared with models of the prototype airplane of the same respec-
tive size.

The Reynolds number range covered by the model tests, along with
certain other pertinent details, is compared with the full-scale air-
planes in table II. Other details can be found in the section entitled
"Models." The area distribution for each of the models is expanded to
its full-scale equivalent and is compared to the full-scale airplanes
in figure 11. As can be seen, the models of the modified airplane are
shorter than the full-scale modified airplane and the cross-sectional
area of the 1/20-scale modified model is greater than the other models
or full scale because the inlets were faired over. For each of the other
models, with open inlets, a mass-flow ratio of 0.9 was assumed, hence 0.9
of the inlet capture area was subtracted from the complete model cross-
sectional area. A mass-flow ratio of 1.0 was assumed in removing inlet
area from the equivalent-body models.

As can be seen in table II, the full-scale data represent the trimmed
condition, whereas the 1/5-scale models have about $1.5°$ of longitudinal
control deflection and the remaining models have none. While there is
no suitable way of adjusting the model data to the respective trim level
of its full-scale counterpart, it is believed that the increment of tran-
sonic drag attributable to the out-of-trim condition of the various models
is probably within the accuracy of the data.

The transonic drag-rise variation with Mach number for the prototype
and the modified airplane is shown in figure 12 for each model and for
the full-scale airplane. In this case the drag rise ΔC_D is defined as
the difference between the minimum drag at Mach numbers above the drag
rise and the minimum drag immediately prior to the drag rise. Part (b)
of figure 12 shows the net improvement provided by the modifications.
The improvement is defined as the difference between ΔC_D for the proto-
type airplane and ΔC_D for the modified airplane. As can be seen, the
improvement as predicted by the 1/20-scale model agrees quite well with
the full-scale results, being approximately 45 drag counts at $M \approx 1.1$.
The improvement as predicted by the 1/5-scale models is about 25 drag
counts at $M \approx 1.1$, while for the equivalent body the improvement is
about 40 counts.

CONCLUSIONS

A comparison of the flight lift and drag characteristics of the
modified airplane and the prototype airplane gave the following results:

1. The anticipated transonic drag reductions associated with the modifications have been realized. The transonic drag rise for the modified airplane is about 0.0050 lower than for the prototype airplane at a Mach number of 1.1. This reduction amounts to about 25 percent of the drag rise for the prototype airplane.

2. Maximum lift-drag ratio for the modified airplane is from 10 to 20 percent higher in the subsonic region and about 15 percent higher in the supersonic region. The modified airplane has slightly lower drag due to lift in the subsonic region.

3. There are significant changes in longitudinal trim which result in less trim drag for the modified airplane. These changes in trim amount to 1^0 to 2^0 less control deflection needed by the modified airplane at moderate lift conditions.

4. Three sets of comparable model data at low Reynolds number indicated reductions in drag coefficient, due to indenting and extending the fuselage, ranging from about 0.0025 to 0.0045 at a Mach number of about 1.1.

High-Speed Flight Station,
      National Advisory Committee for Aeronautics,
            Edwards, Calif., May 9, 1957.

REFERENCES

1. Whitcomb, Richard T.:   A Study of Zero-Lift Drag-Rise Characteristics of Wing-Body Combinations Near the Speed of Sound. NACA Rep. 1273, 1956. (Supersedes NACA RM L52H08.)

2. Saltzman, Edwin J., Bellman, Donald R., and Musialowski, Norman T.: Flight-Determined Transonic Lift and Drag Characteristics of the YF-102 Airplane With Two Wing Configurations. NACA RM H56E08, 1956.

3. Beeler, De E., Bellman, Donald R., and Saltzman, Edwin J.:   Flight Techniques for Determining Airplane Drag at High Mach Numbers. NACA TN 3821, 1956.

TABLE I

TABLE OF PHYSICAL CHARACTERISTICS

	Modified	Prototype
Wing:		
Airfoil section	NACA 0004-65 (Modified)	NACA 0004-65 (Modified)
Total area, sq ft	695.05	695.05
Span (actual), ft	38.17	38.17
Mean aerodynamic chord, ft	23.76	23.76
Root chord, ft	35.63	35.63
Tip chord, ft	0.81	0.81
Taper ratio	0.023	0.023
Aspect ratio	2.08	2.08
Sweep at leading edge, deg	60.1	60.1
Sweep at trailing edge, deg	-5	-5
Incidence, deg	0	0
Dihedral, deg	0	0
Conical camber (leading edge), percent chord	6.3	6.3
Geometric twist, deg	0	0
Inboard fence, percent span	37	37
Outboard fence, percent span	67	67
Tip reflex, deg	6	10
Maximum thickness:		
Root, percent chord	3.9	3.9
Outboard edge of elevon, percent chord	3.5	3.5
Approximate test wing loading, lb/sq ft	35.0	35.0
Elevons:		
Area (total, rearward of hinge line), sq ft	67.2	67.8
Span (one elevon), ft	12.89	13.26
Vertical tail:		
Airfoil section	NACA 0004-65 (Modified)	NACA 0004-65 (Modified)
Area (above waterline 33), sq ft	68.3	68.3
Aspect ratio	1.1	1.1
Sweepback of leading edge, deg	60.0	60.0
Sweepback of trailing edge, deg	-5	-5
Fuselage:		
Length, ft	63.3	52.4
Maximum diameter, ft	6.5	6.5
Total inlet capture area, sq ft	4.6	3.7
Equivalent-body fineness ratio	9.1	6.9
Powerplant:		
Installed static thrust at sea level, lb	8,800	7,400
Installed static thrust at sea level (with afterburner), lb	13,200	11,300
Test center-of-gravity location, percent mean aerodynamic chord	28 to 29	28 to 29

TABLE II

COMPARISON OF PERTINENT PHYSICAL CHARACTERISTICS AND

REYNOLDS NUMBER RANGE FOR THE TEST VEHICLES

Designation	Approximate scale	Internal airflow	Cambered wing	Amount of tip reflex	Center-of-gravity position, percent MAC	Reynolds number $\times 10^{-6}$	δ_e for minimum C_D, deg	Fineness ratio of theoretical equivalent body	Fineness ratio of fuselage only
Airplane:									
Prototype	Full	Yes	Yes	10° up	28 to 29	25 to 77	Trim	6.9	8.5
Modified	Full	Yes	Yes	6° up	28 to 29	30 to 75	Trim	9.1	10.4
Rocket model:									
Prototype	1/5	Yes	No	0	21.9	15 to 39	1.3	6.8	8.5
Modified	1/5	Yes	No	0	22	16 to 45	1.5	8.4	9.5
Wind-tunnel model:									
Prototype	1/20	Yes	Yes	10° up	29.6	4 to 4.8	0	6.5	8.2
Modified	1/20	No	Yes	10° up	29.6	4 to 4.8	0	7.8	8.8
Equivalent-body model:									
Prototype	1/60	Duct area subtracted from body	---	---	---	4 to 8	---	6.9	---
Modified	1/60		---	---	---	4 to 8	---	8.2	---

E-2551
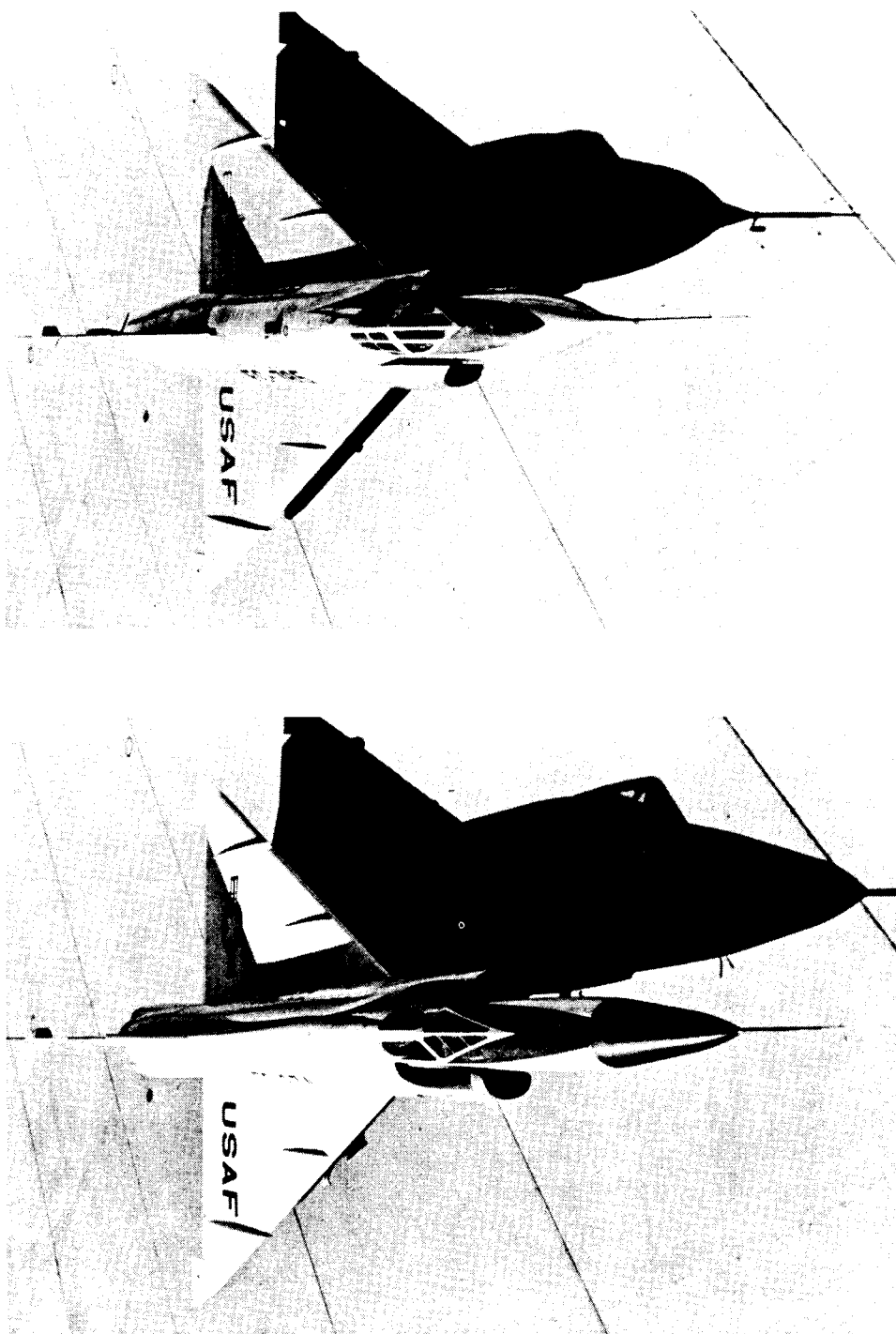
Modified airplane

E-2550

Prototype airplane

(a) Overhead views.

Figure 1.- Photographs of both airplanes.
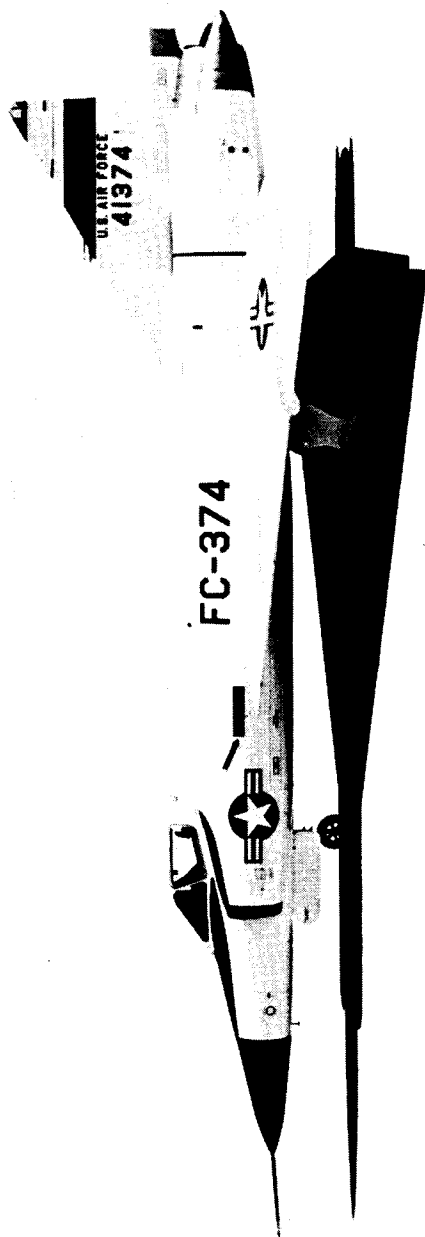
E-2554

Modified airplane
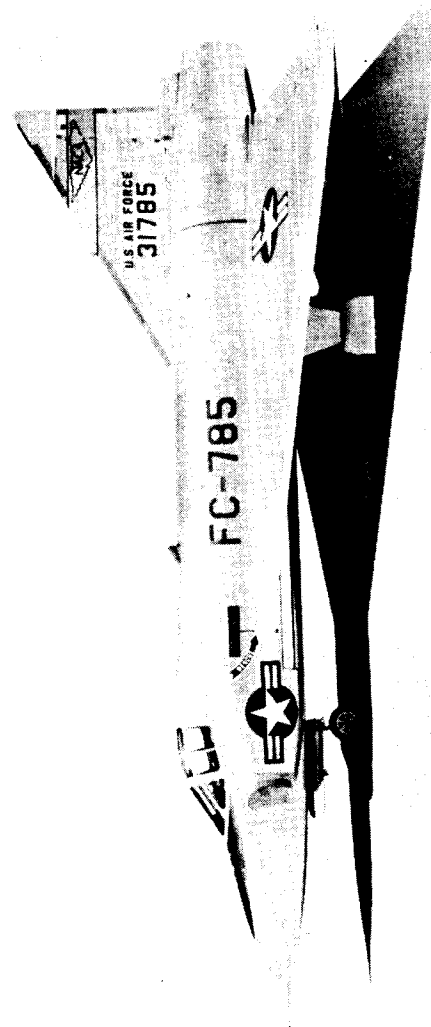
E-1747

Prototype airplane

(b) Side views.

Figure 1.- Concluded.
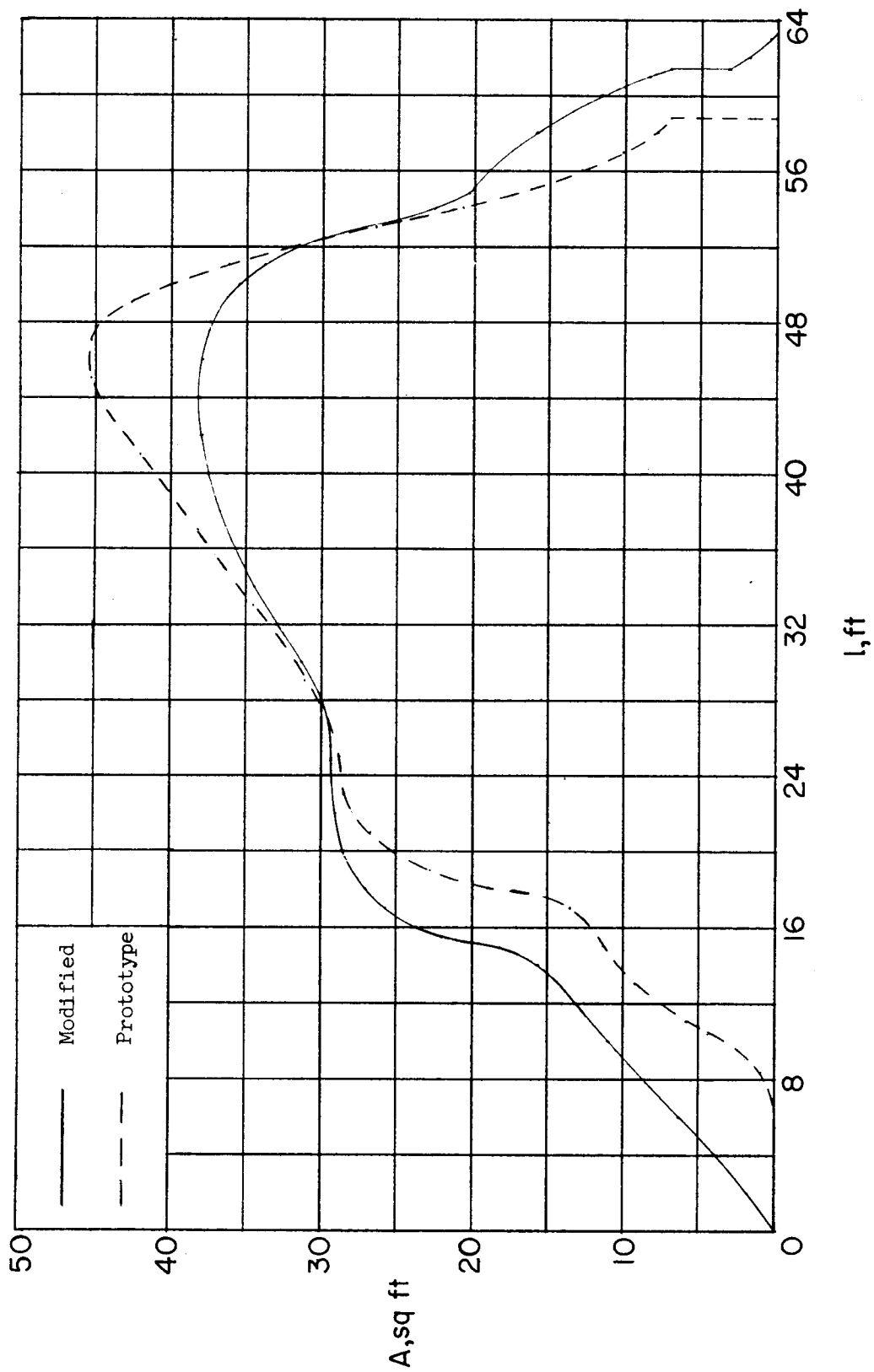
Figure 2.- Cross-sectional-area distribution.
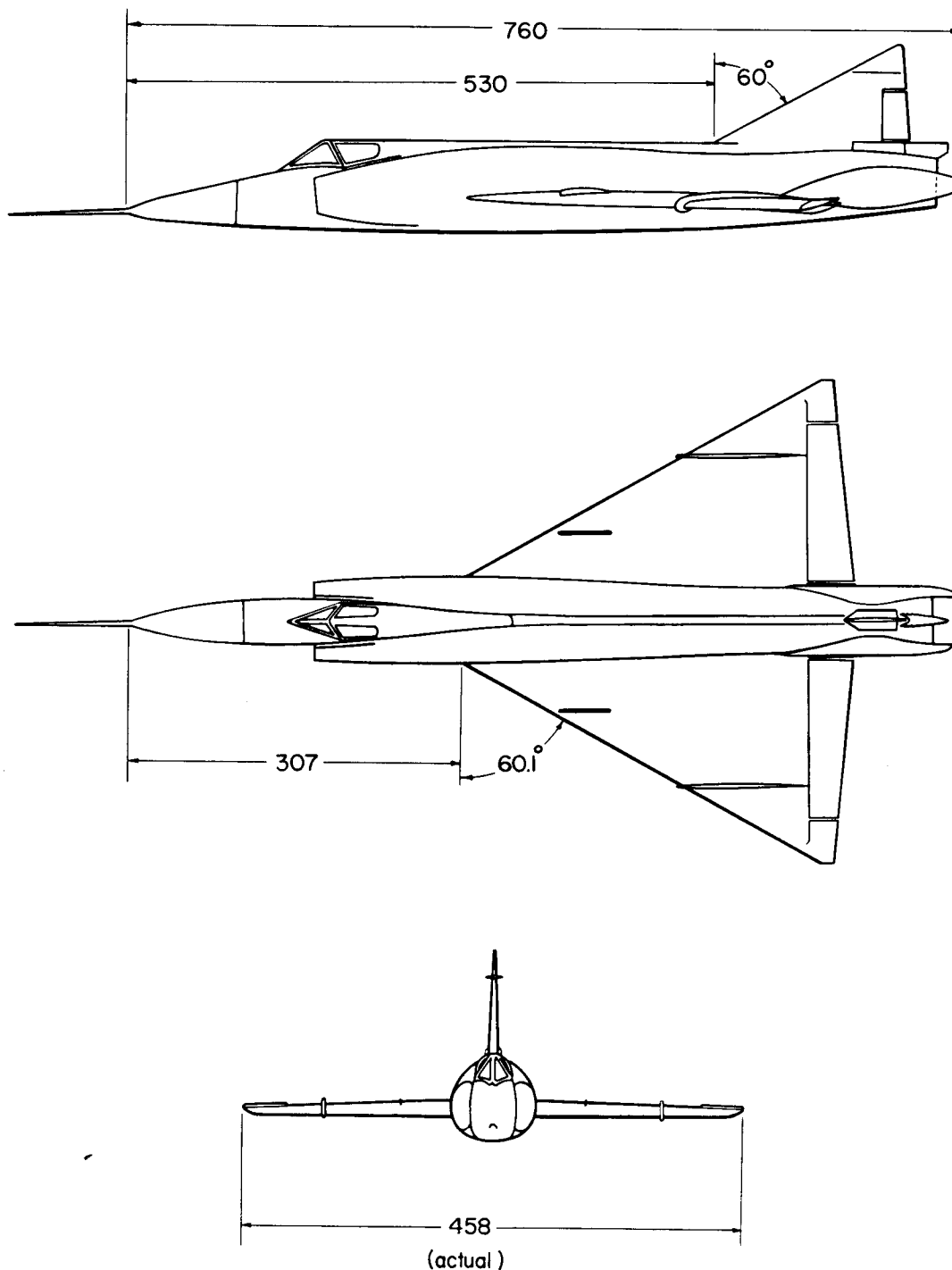
(a) Modified airplane.

Figure 3.- Three-view drawings of both airplanes. All dimensions in inches.
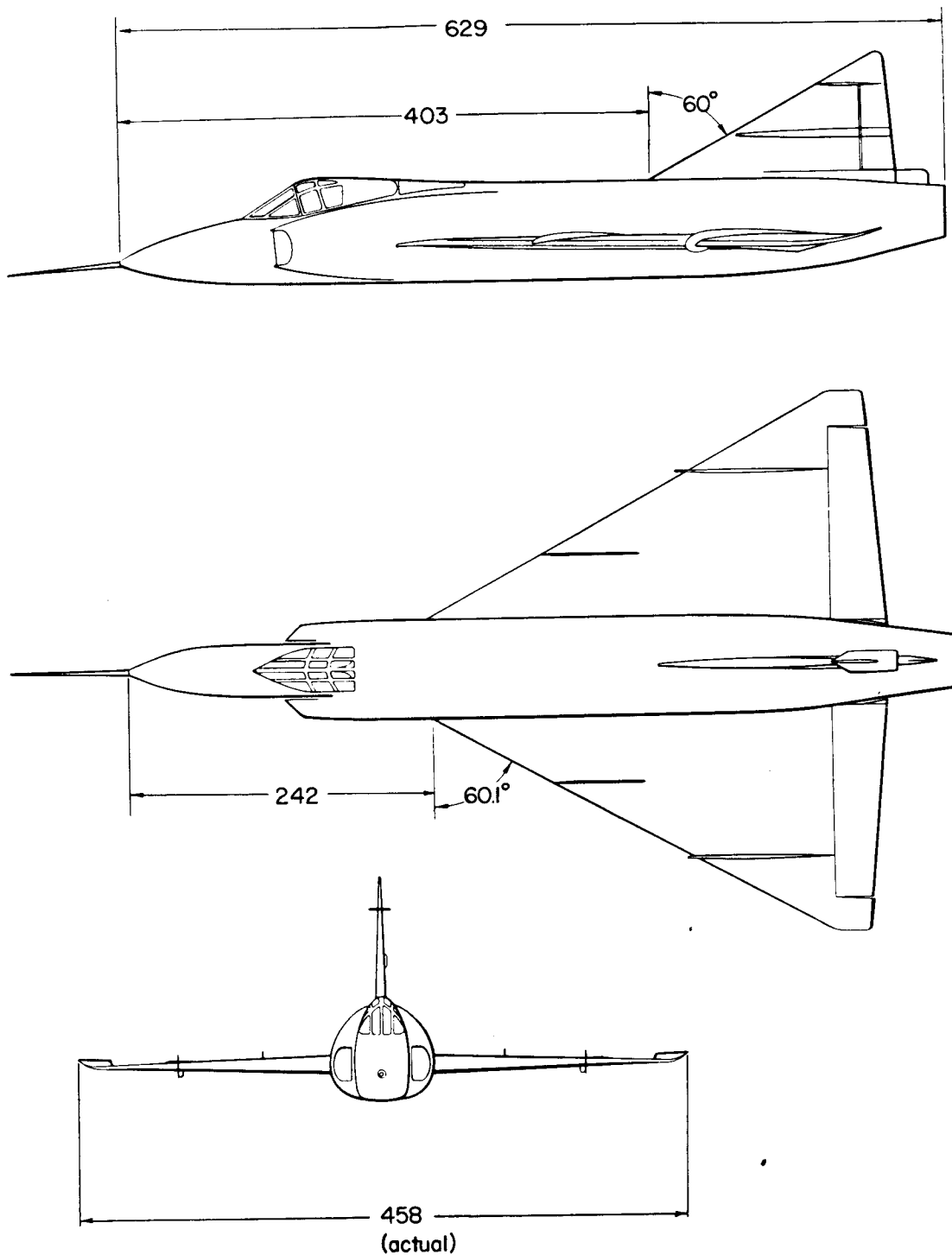
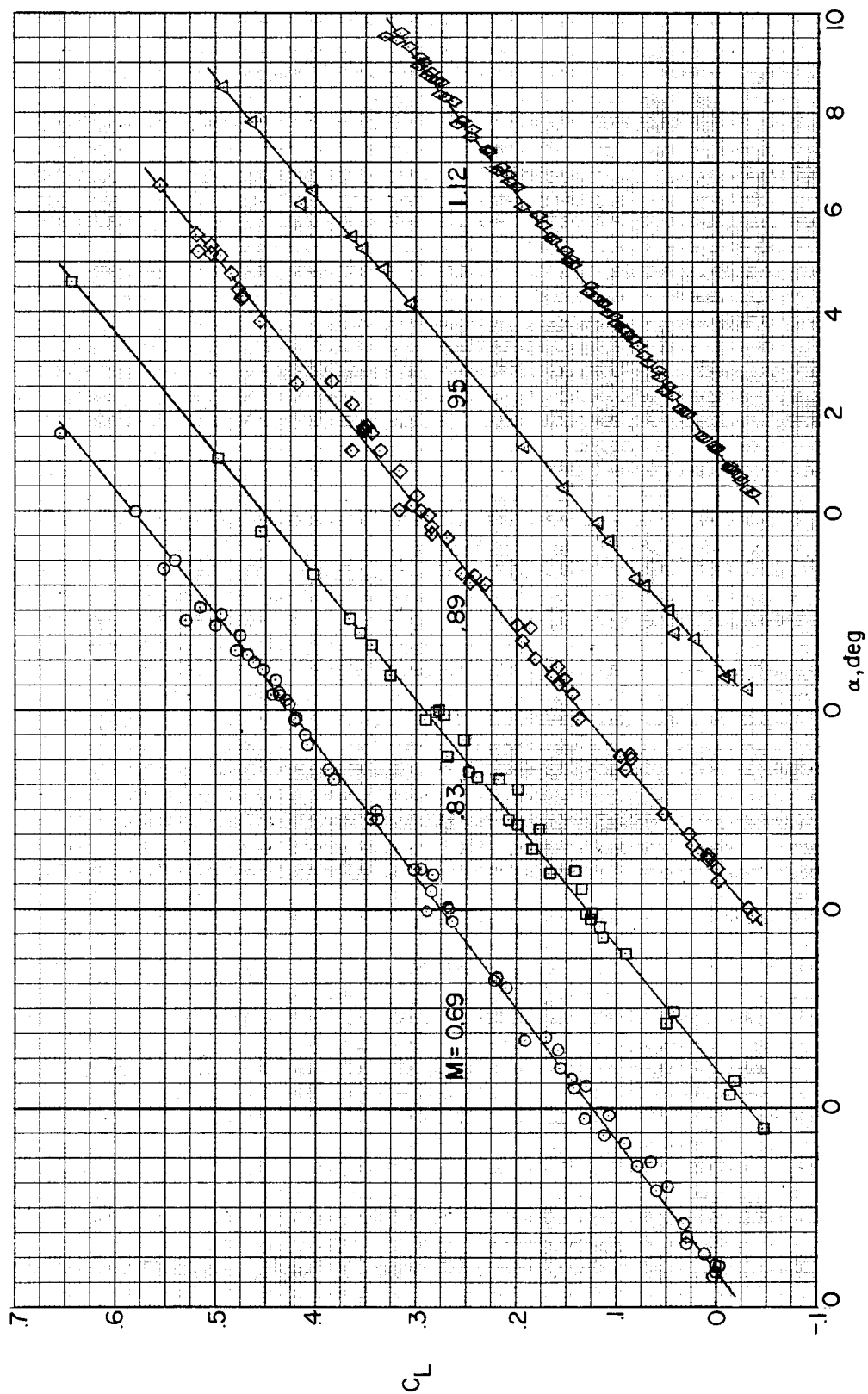(b) Prototype airplane.

Figure 3.- Concluded.

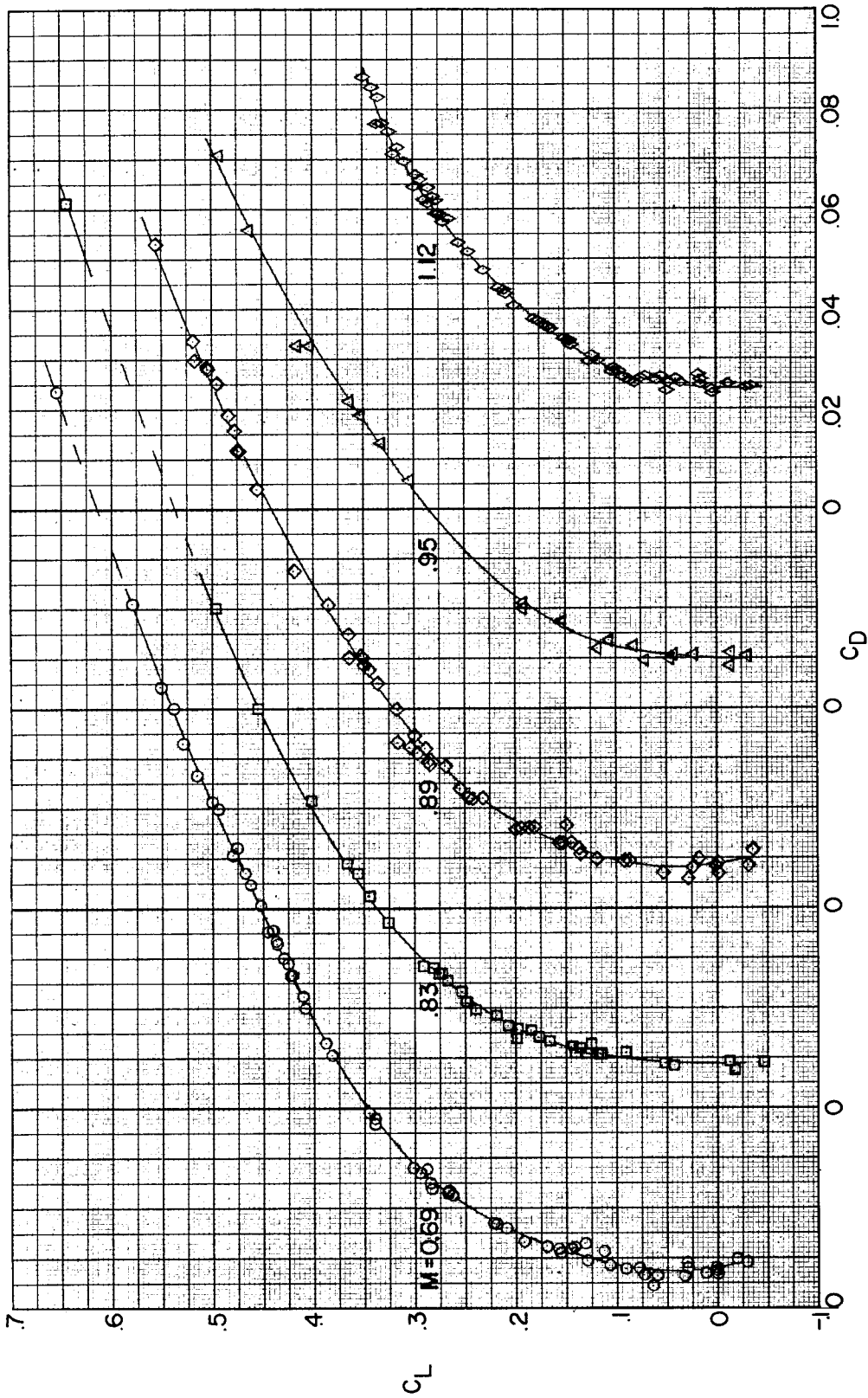Figure 4.- Variation of lift coefficient with angle of attack for the modified airplane. Trimmed flight.

Figure 5.- Variation of drag coefficient with lift coefficient for the modified airplane. Trimmed flight.

CONFIDENTIAL   NACA RM H57E29
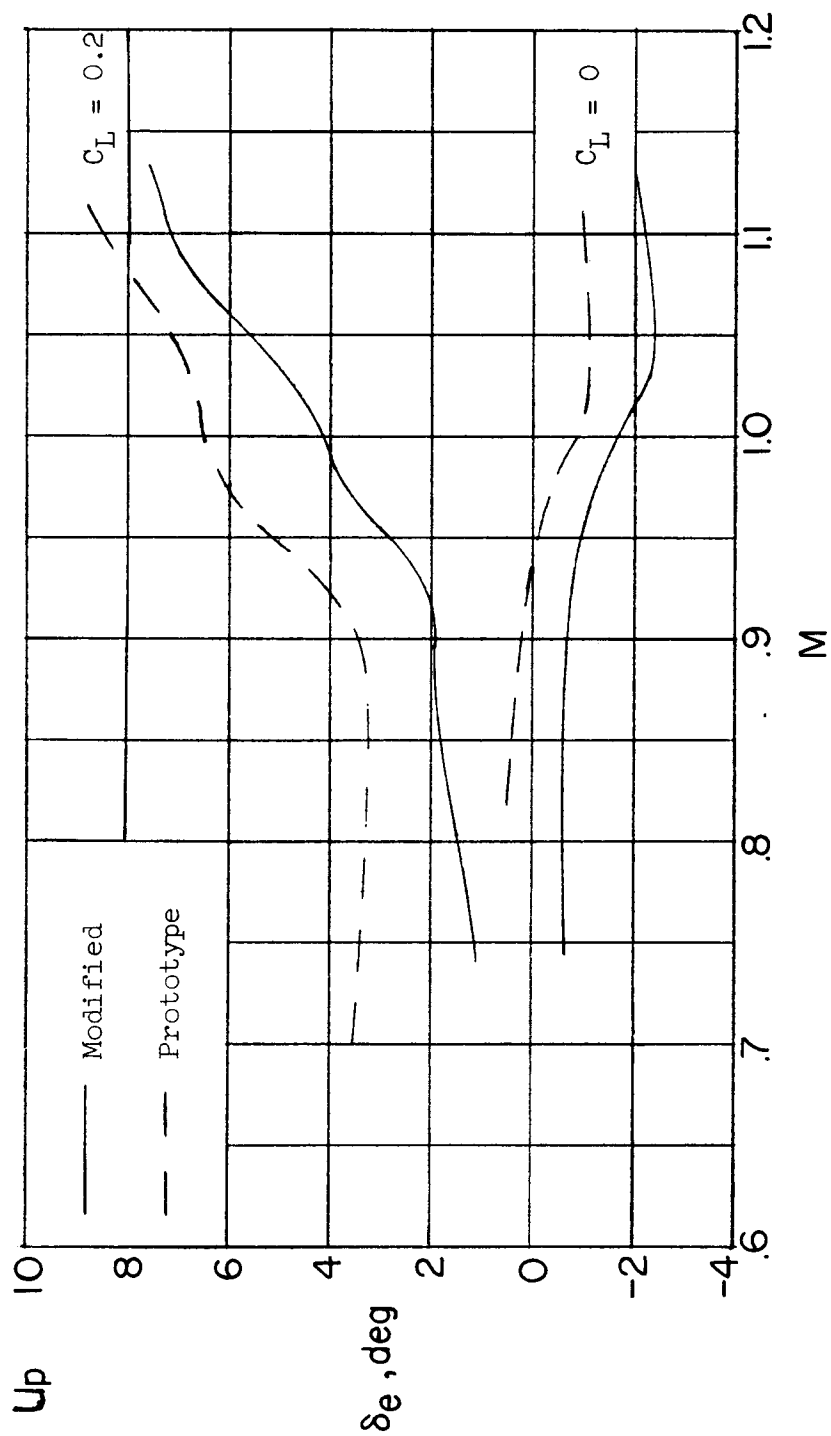
Figure 6.- Flight trim characteristics.
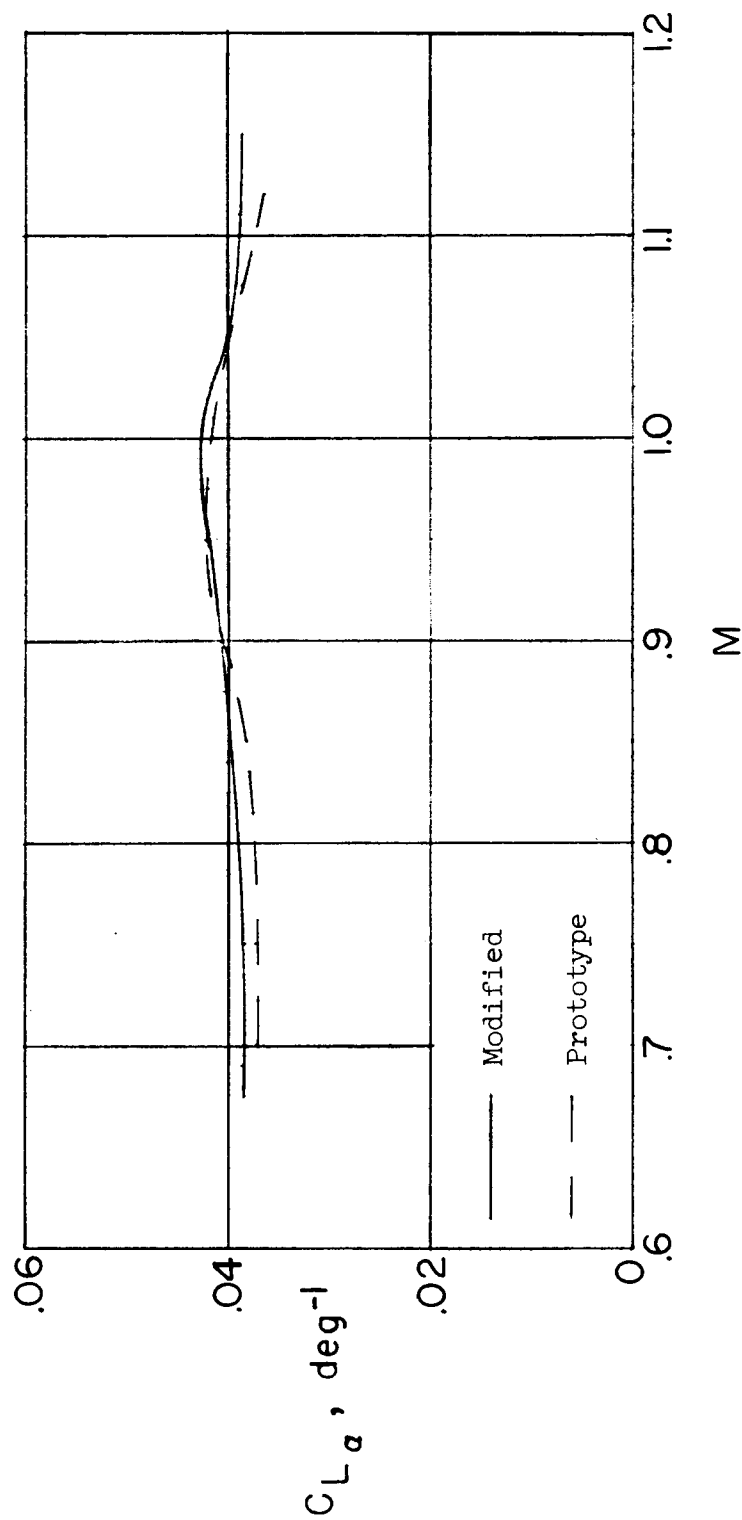
Figure 7.- Variation of the lift-curve slope with Mach number. $C_L \leqq 0.3$. Trimmed flight.
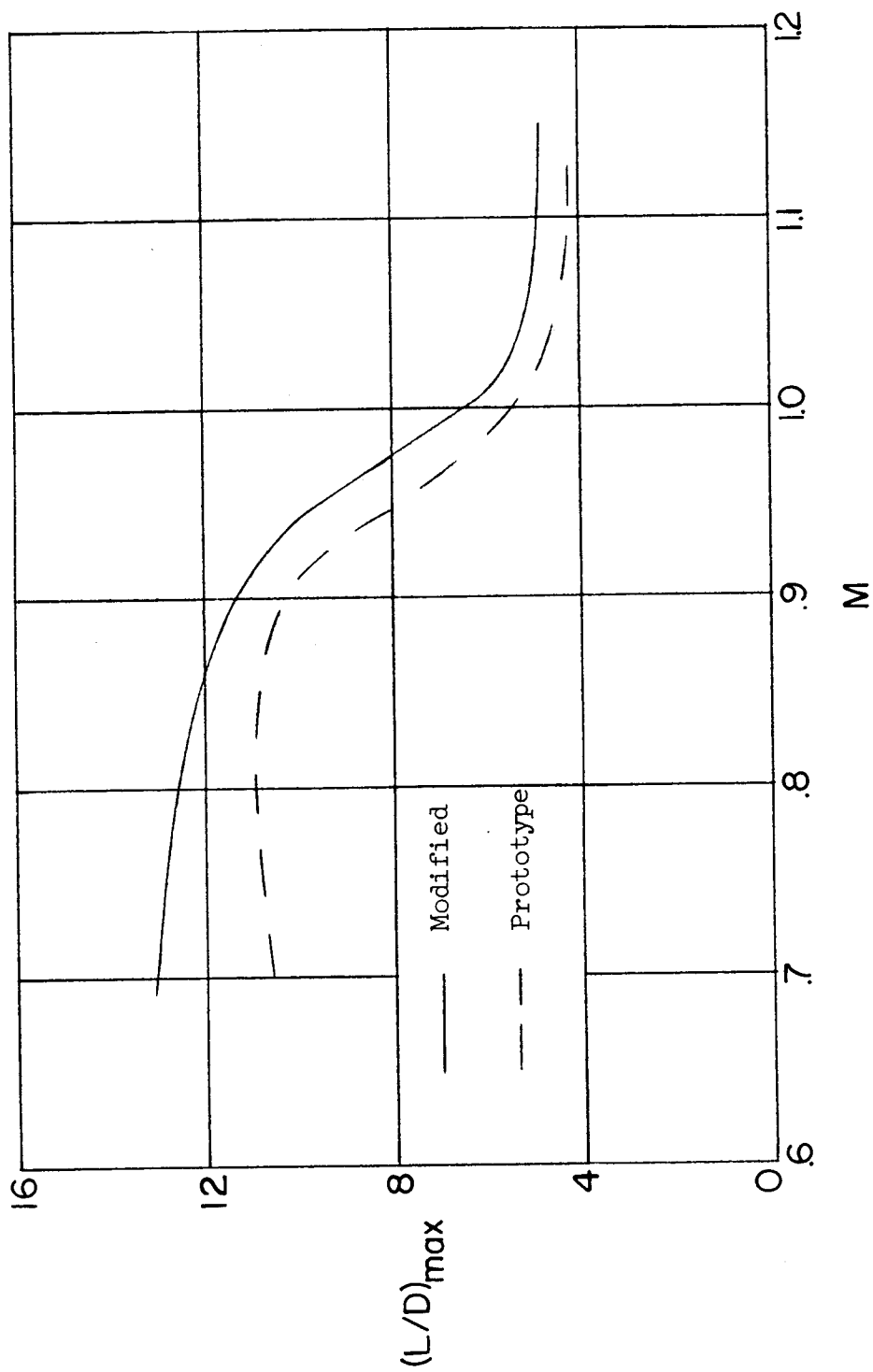
Figure 8.- Variation of maximum lift-drag ratio with Mach number. Trimmed flight.
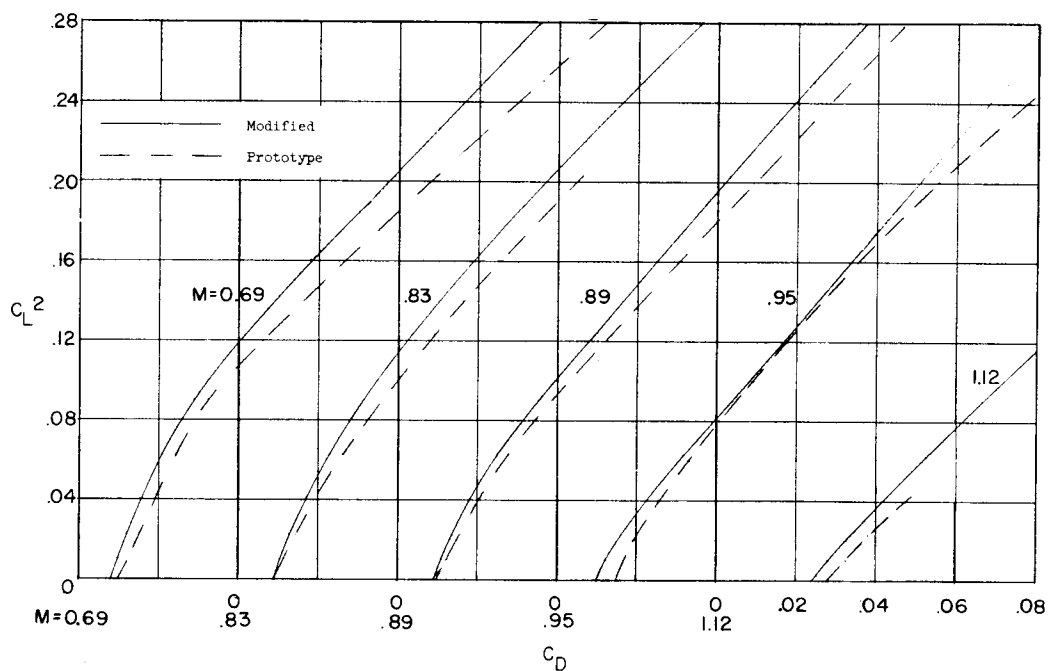
(a) Variation of C_L^2 with C_D.
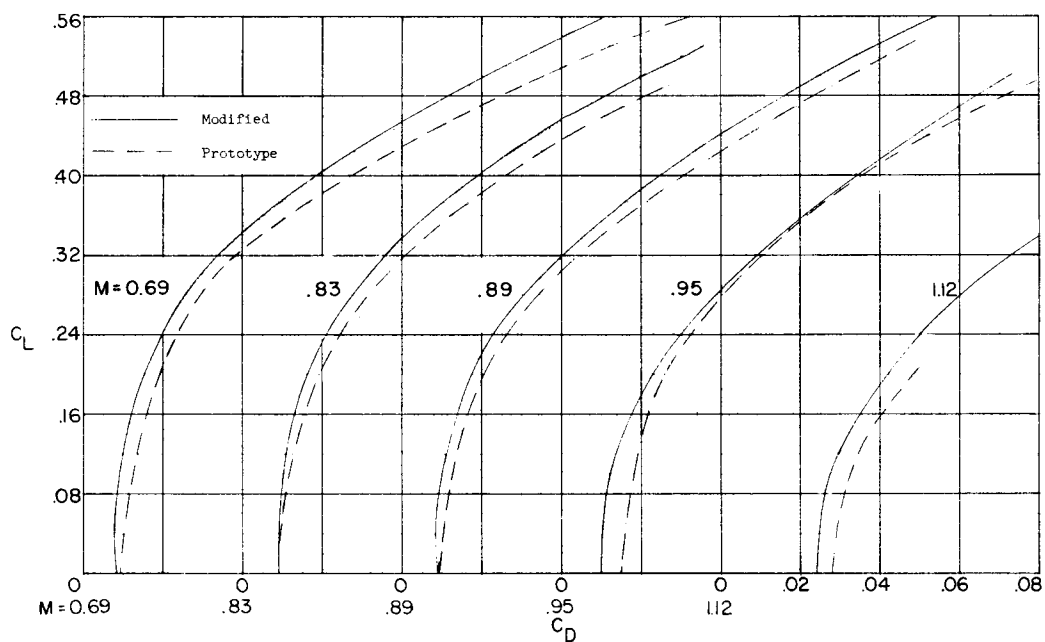
(b) Variation of C_L with C_D.

Figure 9.- Comparison of lift-drag relationship at selected Mach numbers. Trimmed flight.
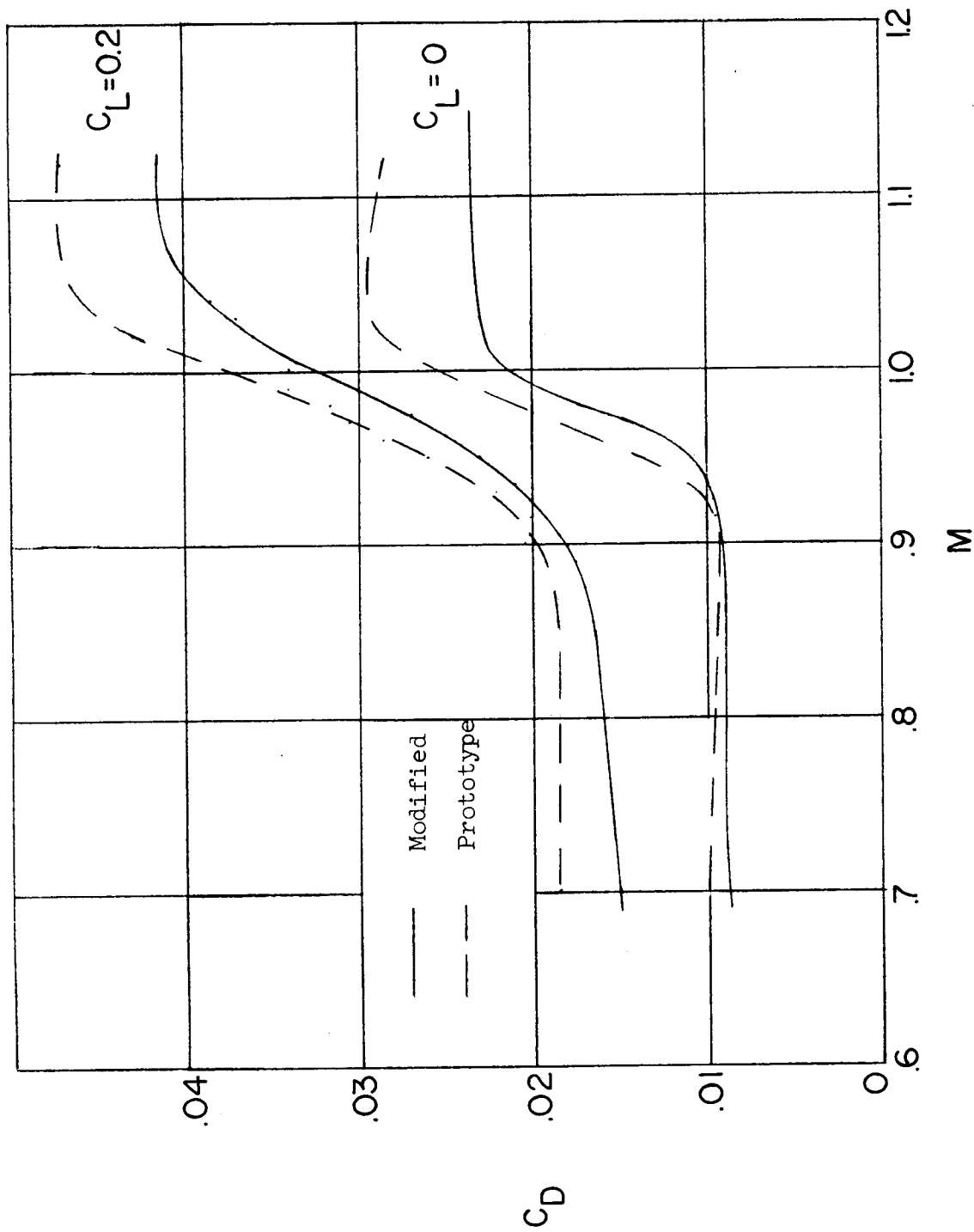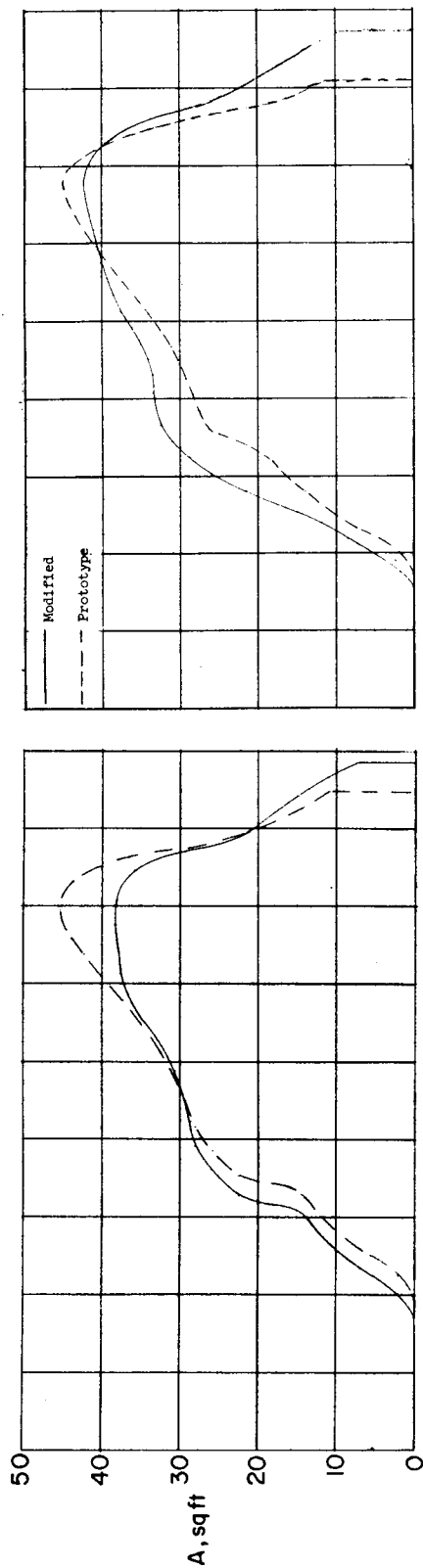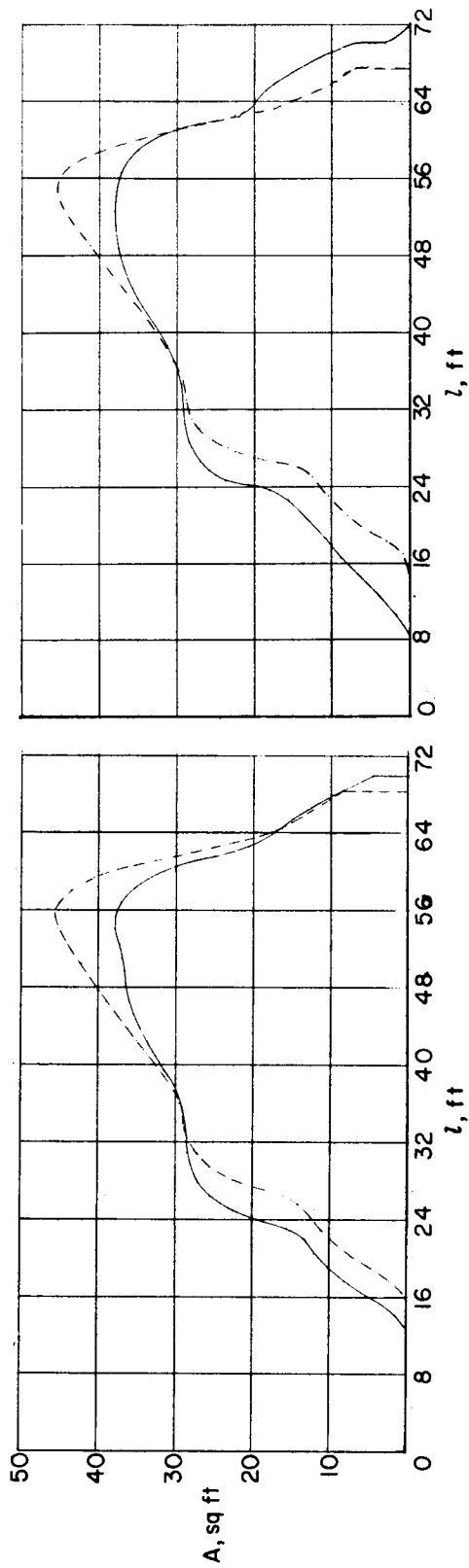
Figure 10.- Variation of drag coefficient with Mach number. Trimmed flight.
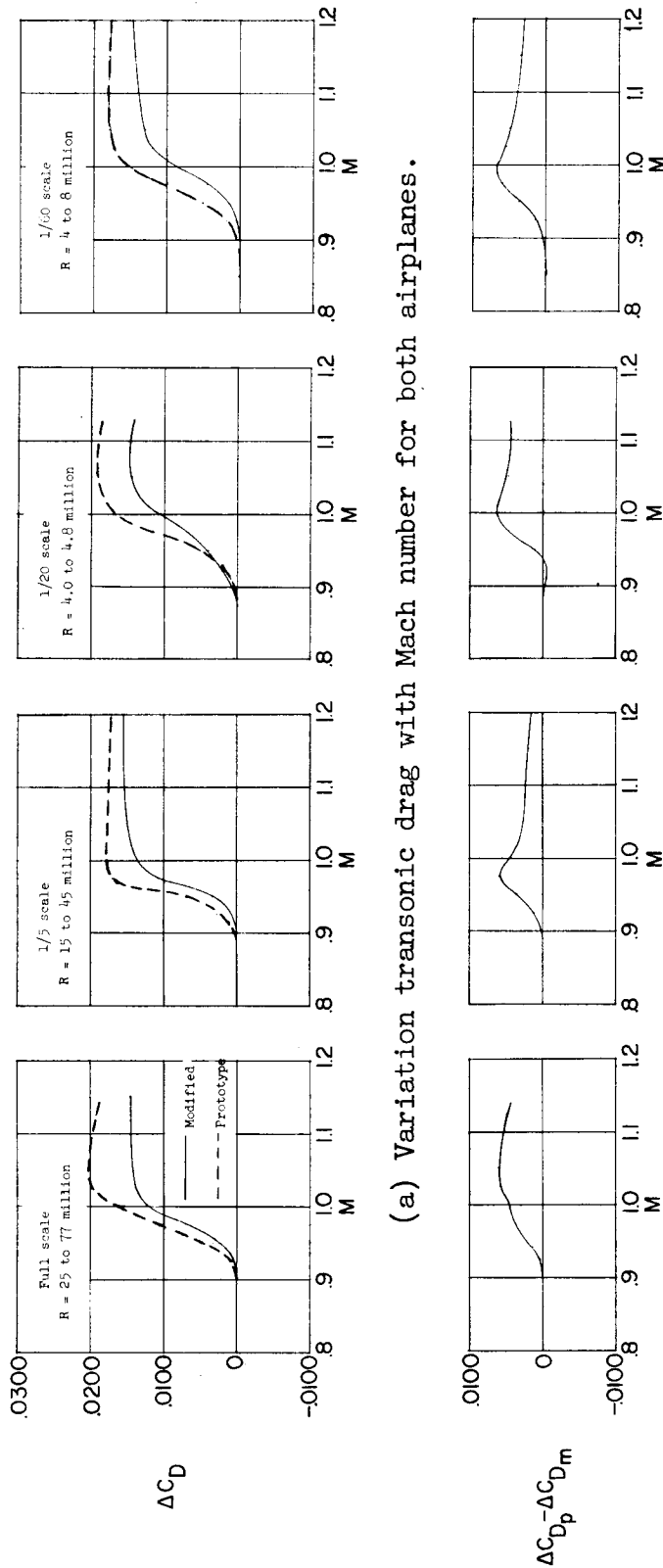
(a) Equivalent-body models.

(b) 1/20-scale models.

(c) 1/5-scale models.

(d) Full-scale airplanes.

Figure 11.- Cross-sectional-area distribution for equivalent-body models, 1/20-scale and 1/5-scale models, and full-scale airplanes.

(a) Variation transonic drag with Mach number for both airplanes.

(b) Difference in transonic drag coefficient increment between prototype airplane and modified airplane.

Figure 12.- Transonic drag characteristics of prototype airplane and modified airplane for full-scale airplane, 1/5-scale and 1/20-scale models, and equivalent-body models.

NACA - Langley Field, Va.